Available online at www.sciencedirect.com
SCIENCE DIRECT®
International Journal of Mass Spectrometry 227 (2003) 563–575
International Journal of Mass Spectrometry
www.elsevier.com/locate/ijms

Kinetics and thermodynamics for the bonding of benzene to 20 main-group atomic cations: formation of half-sandwiches, full-sandwiches and beyond

Gregory K. Koyanagi, Diethard K. Bohme*

Department of Chemistry, Centre for Research in Mass Spectrometry and Centre for Research in Earth and Space Science, York University, Toronto, Ont., Canada M3J 1P3

Received 8 April 2002; accepted 12 September 2002

Abstract

An inductively coupled plasma/selected-ion flow tube (ICP/SIFT) tandem mass spectrometer has been employed in a systematic study of room-temperature reactions of benzene (C_6H_6 or C_6D_6) with 20 main-group atomic cations (non-transition metals). These include the Group 1 ions K^+, Rb^+ and Cs^+, the Group 2 ions Ca^+, Sr^+ and Ba^+, the Group 12 ions Zn^+, Cd^+, and Hg^+, the Group 13 ions Ga^+, In^+ and Tl^+, the Group 14 ions Ge^+, Sn^+ and Pb^+, the Group 15 ions As^+, Sb^+ and Bi^+, the Group 16 ion Te^+ and the Group 17 ion I^+. The atomic ions were produced at ca. 5500 K in a plasma ion source and allowed to decay radiatively and to thermalize by collisions with Ar and He atoms prior to reaction in He at 0.35 Torr and 296 K. Benzene addition was observed to proceed rapidly, $k > 3 \times 10^{-10}$ cm^3 molecule^{-1} s^{-1} with most ions. Hg^+ and I^+ reacted by electron transfer and electron transfer was observed to compete with addition (in a ratio of 1:3) in the reaction with Zn^+. Most of the other cations added two benzene molecules, but the larger Group 2 (s^1) ions Ca^+, Sr^+ and Ba^+ added three benzene molecules in rapid succession. Equilibrium was achieved among the first additions only for Group 1 cations and for most of the second benzene additions that were observed. Standard free energy changes derived from the corresponding equilibrium constants are reported and compared with predictions based on B3LYP density functional theory. Both the experiments and theory show a large free energy change for the first ligation with benzene (more negative than -14 kcal mol^{-1}), except for the Group 1 cations which have a rare-gas electronic configuration. A large decrease in the absolute free energy change for the addition of the second molecule of benzene is also observed. Theory has provided structural parameters for half- and full-sandwich structures and periodic trends in these structures are rationalized in terms of the valence shell electron (VSEC) configuration of the atomic ion.

Keywords: Main-group atomic cations; Benzene; Ligation; Kinetics; Thermodynamics

1. Introduction

The thermochemistry, structural chemistry and biochemistry of atomic cation–π interactions involving benzene have been receiving growing attention in recent years, particularly since benzene has become a prototype aromatic molecule in the study of cation–π

* Corresponding author. Tel.: +1-416-736-2100x66188; fax: +1-416-736-5936.
E-mail address: dkbohme@yorku.ca (D.K. Bohme).

1387-3806/03/$ – see front matter © 2003 Elsevier Science B.V. All rights reserved.
doi:10.1016/S1387-3806(03)00091-5

interactions that determine the structures of biomolecules [1]. The very recent detection of benzene in circumstellar environments also reinforces the possible importance of the organometallic chemistry of benzene in the interstellar medium where it may serve as a sink for metal ions [2,3].

Among the main-group atomic cations, alkali-metal cations have received the most attention so far in studies of their interactions with benzene. Early work by Wooden and Beauchamp [4] using ICR techniques and Kebarle et al. [5] using high-pressure ion source mass spectrometry focussed on the determination of the thermodynamics of benzene ligation of Li^+ and K^+, respectively, with equilibrium constant measurements and theory. Especially noteworthy is the reported observation by Kebarle et al. [5] of equilibria for the addition of up to four benzene molecules to K^+ over a wide range in temperature. The fourth adduct was observed only below 280 K. Later Castleman reported high-pressure reaction cell measurements of equilibrium constants as a function of temperature for the single ligation of Na^+ and Pb^+ with benzene [6]. Very recently, Amicangelo and Armentrout [7] reported the determination of the absolute bond energies of both mono- and bis-benzene adducts with almost all of the alkali cations (Li^+, Na^+, K^+, Rb^+ and Cs^+) using threshold collision-induced dissociation experiments and ab initio theory. Also, the geometries and binding enthalpies of adducts of benzene with the same alkali ions were obtained by Dixon, Nicholas and co-workers [8,9] from large basis set second-order perturbation theory and coupled cluster theory calculations.

The interactions of main-group ions other than the alkali ions with benzene have received considerably less attention. Reactions of Zn^+, Cd^+ and Hg^+ with benzene have been investigated previously at the low pressures of a FT-ICR mass spectrometer [10]. The time dependence of the ionic evolution due to sequential reaction was monitored, but rate coefficients were not deduced. The major reaction observed with Zn^+ and Hg^+ was electron transfer, while Cd^+ was observed to add one molecule of benzene. The attachment of In^+ to benzene to form the half-sandwich was investigated for the first time, both experimentally and theoretically, in the context of its application in ion-attachment mass spectrometry by Arulmozhitaja and Fujii [11,12]. In the experimental studies In^+ was generated by thermionic emission.

In the experimental and theoretical study reported here, we have surveyed the kinetics and energetics of reactions of benzene with 20 main-group atomic ions in Groups 12–17 on the periodic table, as well as Groups 1 and 2. The experimental technique that has been employed is sufficiently versatile to provide both kinetic and equilibrium measurements. The theoretical approach was at a level sufficient to provide structural information and moderately accurate thermochemical parameters.

1.1. Experimental method

The results reported here were obtained using the selected-ion flow tube (SIFT) tandem mass spectrometer in the Ion-Chemistry Laboratory at York University, described in detail elsewhere [13,14]. Recently, it has been modified to accept ions generated in an inductively coupled plasma (ICP) torch through an atmosphere/vacuum interface (ELAN series, Perkin Elmer SCIEX). The ICP ion source and interface have also been described previously [15,16]. Solutions containing the metal salt of interest were peristatically pumped via a nebulizer into the plasma. The nebulizer flow was adjusted to maximize the ion signal detected downstream of the SIFT. The sample solutions were prepared using atomic spectroscopy standard solutions commercially available from SPEX, Teknolab, J.T. Baker Chemical Co., Fisher Scientific Company, Perkin-Elmer and Alfa Products. Aliquots of standard solutions were diluted with highly purified water produced in the Millipore Milli-Qplus ultra-pure water system. The final concentrations were varied from 5 to 20 ppm to achieve suitable intensity of the resultant ion beam. Normally, a stabilizing agent was added to each solution to prevent precipitation. That was either HNO_3 or HCl for acid-stabilized salts, and KOH for those base-stabilized.

The transition-metal ions emerge from the plasma at a nominal plasma temperature of 5500 K. After

extraction from the ICP the plasma ions may experience both radiative electronic-state relaxation and collisional electronic-state relaxation. The latter may occur with argon as the extracted plasma cools upon sampling and then by collisions with He atoms in the flow tube (ca. 4×10^5 collisions) prior to the reaction region, but the actual extent of electronic relaxation (either radiative or collisional) is not known. The collisions with He ensure that the ions reach a translational temperature equal to the tube temperature of 295 ± 2 K prior to entering the reaction region. The helium buffer gas pressure was 0.35 ± 0.01 Torr. Benzene, obtained from Sigma (C_6H_6: +99.9%, C_6D_6: 99.6 atm%) was introduced into the flow tube as a ca. 10% solution in He.

Reaction rate coefficients were determined in the usual manner using pseudo first-order kinetics [13,14]. The rate coefficients for the primary reactions reported herein have an absolute accuracy of ±30%; those for higher-order additions have an absolute accuracy of better than ±50%.

The multicollision-induced dissociation (MCID) of sampled ions is investigated by changing the potential of the sampling nose cone from 0 to −80 V [17]. Thresholds for dissociation are obtained from plots of relative ion intensities as a function of accelerating voltage and these provide insight into bond connectivities.

1.2. Theoretical method

Ion structures, reaction enthalpies, and reaction free energies were computed for the binding of K^+, Ca^+, Zn^+ through Se^+, Rb^+, Sr^+ and Cd^+ through Te^+ with one and two benzene molecules. Computations were performed using Gaussian 98 [18]. The density functional method denoted as B3LYP consisting of Becke's three-parameter exchange functional [19] combined with the correlation functional of Lee, Yang and Parr was utilized [20,21]. Salahub's DZVP basis set was used for all nuclear centers [22].[1] Computed harmonic vibrational frequencies were utilized un-scaled. The synchronous torsional vibration of benzene molecules in the $M(C_6H_6)_2^+$ clusters was treated as a free internal rotation and typically accounted for 9 cal mol^{-1} K^{-1} of entropy in the sandwich cluster.

2. Results and discussion

The reactions of 20 main-group atomic metal ions were investigated with benzene (C_6H_6/C_6D_6). These include the Group 1 ions K^+, Rb^+ and Cs^+, the Group 2 ions Ca^+, Sr^+ and Ba^+, the Group 12 ions Zn^+, Cd^+, and Hg^+, the Group 13 ions Ga^+, In^+ and Tl^+, the Group 14 ions Ge^+, Sn^+ and Pb^+, the Group 15 ions As^+, Sb^+ and Bi^+, the Group 16 ion Te^+ and the Group 17 ion I^+.

The predominant feature of the observed chemistry was sequential addition of two benzene molecules according to reactions (1) and (2).

$$M^+ + C_6H_6 \rightarrow MC_6H_6^+ \quad (1)$$

$$MC_6H_6^+ + C_6H_6 \rightarrow M(C_6H_6)_2^+ \quad (2)$$

The Group 3 ions Ca^+, Sr^+ and Ba^+ were observed to add a third benzene molecule according to reaction (3).

$$M(C_6H_6)_2^+ + C_6H_6 \rightarrow M(C_6H_6)_3^+ \quad (3)$$

Reactions (1)–(3) are presumed to occur in a termolecular fashion with He acting as the stabilizing third body. The reactions were not measured as a function of pressure so that the possible contribution of radiative association could not be ascertained. Electron transfer, reaction (4), was observed to be the only competing primary reaction channel.

$$M^+ + C_6H_6 \rightarrow M + C_6H_6^+ \quad (4)$$

[1] Basis sets were obtained from the Extensible Computational Chemistry Environment Basis Set Database, Version 2/25/02, as developed and distributed by the Molecular Science Computing Facility, Environmental and Molecular Sciences Laboratory which is part of the Pacific Northwest Laboratory, P.O. Box 999, Richland, Washington 99352, USA, and funded by the U.S. Department of Energy. The Pacific Northwest Laboratory is a multi-program laboratory operated by Battelle Memorial Institue for the U.S. Department of Energy under contract DE-AC06-76RLO 1830. Contact David Feller or Karen Schuchardt for further information.

Of the atomic cations studied, electron transfer from benzene (I.E. = 9.24378 eV [23]) is exothermic for Hg^+ (IE(Hg) = 10.4375 eV [24]), I^+ (IE(I) = 10.4513 eV [25]) and Zn^+ (IE(Zn) = 9.3942 eV [26]). Electron transfer, exclusively, was observed with Hg^+ and I^+, while both electron transfer and benzene addition was observed with Zn^+ in the ratio of 1:3.

2.1. Reaction kinetics

Table 1 summarizes the observed reaction kinetics and presents the corresponding reaction efficiencies. The reaction efficiency is taken to be equal to the ratio k/k_c where k is the experimentally measured rate coefficient and k_c is the capture or collision rate coefficient computed using the algorithm of the modified variational transition-state/classical trajectory theory developed by Su and Chesnavich [27].

For many of the main-group ions, the effective bimolecular rate coefficient for attachment at 0.35 Torr and 296 K is quite large, $k > 3 \times 10^{-10}$ cm^3 molecule^{-1} s^{-1}, and the corresponding efficiencies, k/k_c, are >0.28. In the case of the Group 1 ions K^+, Rb^+ and Cs^+, weak bonding with benzene and the consequent occurrence of the reverse reaction and approach to equilibrium allowed only the determination of lower limits to the rate coefficients for benzene attachment. There were no obvious trends in the rate coefficient for attachment with electronic configuration of the atomic ion, except perhaps for the systematic decrease in rate going down the periodic table observed with the Group

Table 1
Apparent bimolecular reaction rate coefficients and reaction efficiencies obtained under ICP/SIFT conditions (0.35 Torr He, 296 K) for the reactions of benzene with main-group atomic cations

Ion	$MC_6H_6^+$ formation		$M(C_6H_6)_2^+$ formation		Extent of clustering[a]
	k[b]	k/k_c[c]	k[b]	k/k_c[c]	
K^+	>0.040	>0.027	>0.040	>0.037	2
Rb^+	>0.013	>0.011	>0.0017	>0.0016	2 (3)
Cs^+	>0.012	>0.011	NA	NA	1 (2)
Ca^+	0.35	0.24	0.70	0.65	3
Sr^+	0.26	0.22	0.61	0.60	3
Ba^+	0.62	0.61	0.75	0.77	3
Zn^+	0.97	0.78	0.28	0.27	2, e^- transfer[d]
Cd^+	0.41	0.39	0.21	0.21	2
Hg^+	0.87	0.88	NA	NA	e^- transfer
Ga^+	1.17	0.96	>0.029	>0.028	2
In^+	0.44	0.41	>0.021	>0.021	2
Tl^+	0.27	0.28	>0.017	>0.018	2
Ge^+	0.95	0.79	>0.033	>0.032	2
Sn^+	0.85	0.79	>0.077	>0.078	2
Pb^+	0.46	0.47	>0.039	>0.041	2
As^+	0.55	0.46	NA	NA	1 (2)
Sb^+	0.76	0.71	>0.033	>0.033	2
Bi^+	0.61	0.62	>0.065	>0.069	2
Te^+	0.82	0.77	>0.029	>0.029	2
I^+	0.62	0.59	NA	NA	e^- transfer

[a] Numbers in parentheses indicate that an adduct peak was observed in the mass spectrum but was too weak for use in accurate kinetic measurements.

[b] Effective bimolecular rate coefficient in units of 10^{-9} cm^3 molecule^{-1} s^{-1}. The estimated accuracy is ±30% for the primary addition and up to ±50% for the secondary addition. NA indicates that data could not be fit to provide k or that electron transfer was observed for the primary reaction instead of benzene addition.

[c] Reaction efficiency. The capture rate coefficient k_c is computed (see text) assuming a value of 10×10^{-24} cm^3 for the polarizability of benzene.

[d] Branching ratio for clustering versus electron transfer is 3:1.

13 ions Ga^+, In^+ and Tl^+ and the Group 14 ions Ge^+, Sn^+ and Pb^+.

The number of sequential additions of benzene that were observed was generally 2. This is illustrated in Fig. 1 for the reactions of the Group 14 ions Ge^+, Sn^+ and Pb^+. Rate coefficients for the second benzene addition could be obtained for the Group 2 ions Ca^+, Sr^+ and Ba^+ and the Group 12 ions Zn^+ and Cd^+ and these are included in Table 1. In the remaining cases, again because of weak bonding with benzene and the consequent occurrence of the reverse reaction and approach to equilibrium, only lower limits could

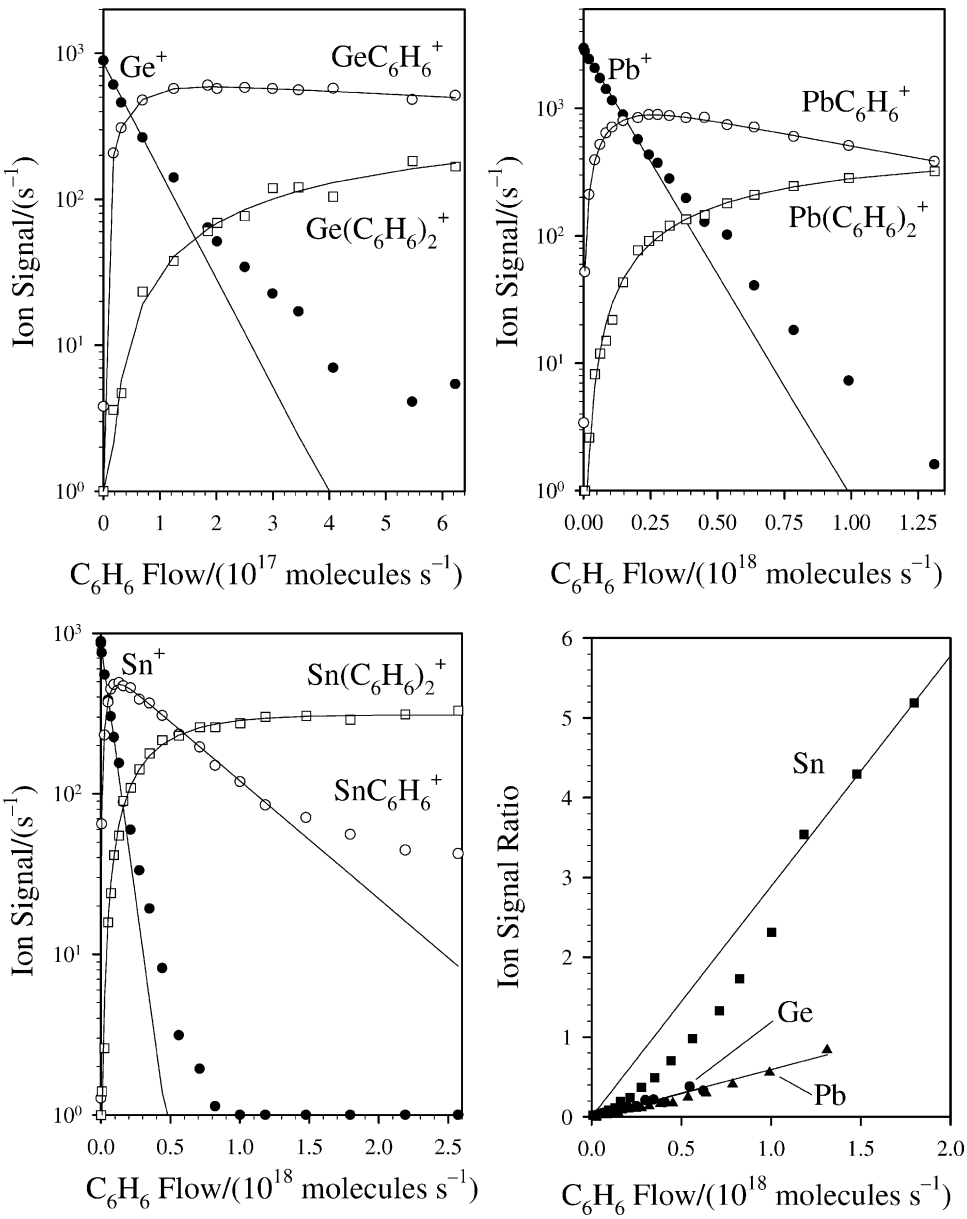

Fig. 1. Reaction profiles for the reactions of Ge^+, Sn^+, and Pb^+ reacting with benzene to form $M(C_6H_6)_2^+$ clusters by sequential addition. Ion signal ratio-plots (lower right) show the variation in $M(C_6H_6)_2^+/MC_6H_6^+$ with the flow of benzene.

be obtained for the rate coefficient for the attachment of the second benzene molecule (see Table 1).

The Group 2 (s^1) ions Ca^+, Sr^+ and Ba^+ exhibited an exceptional behaviour in that they added three benzene molecules in rapid succession. Experimental results obtained for this chemistry are shown in Fig. 2. The effective bimolecular rate coefficients for the three sequential additions are 3.5 and 7.0 ×

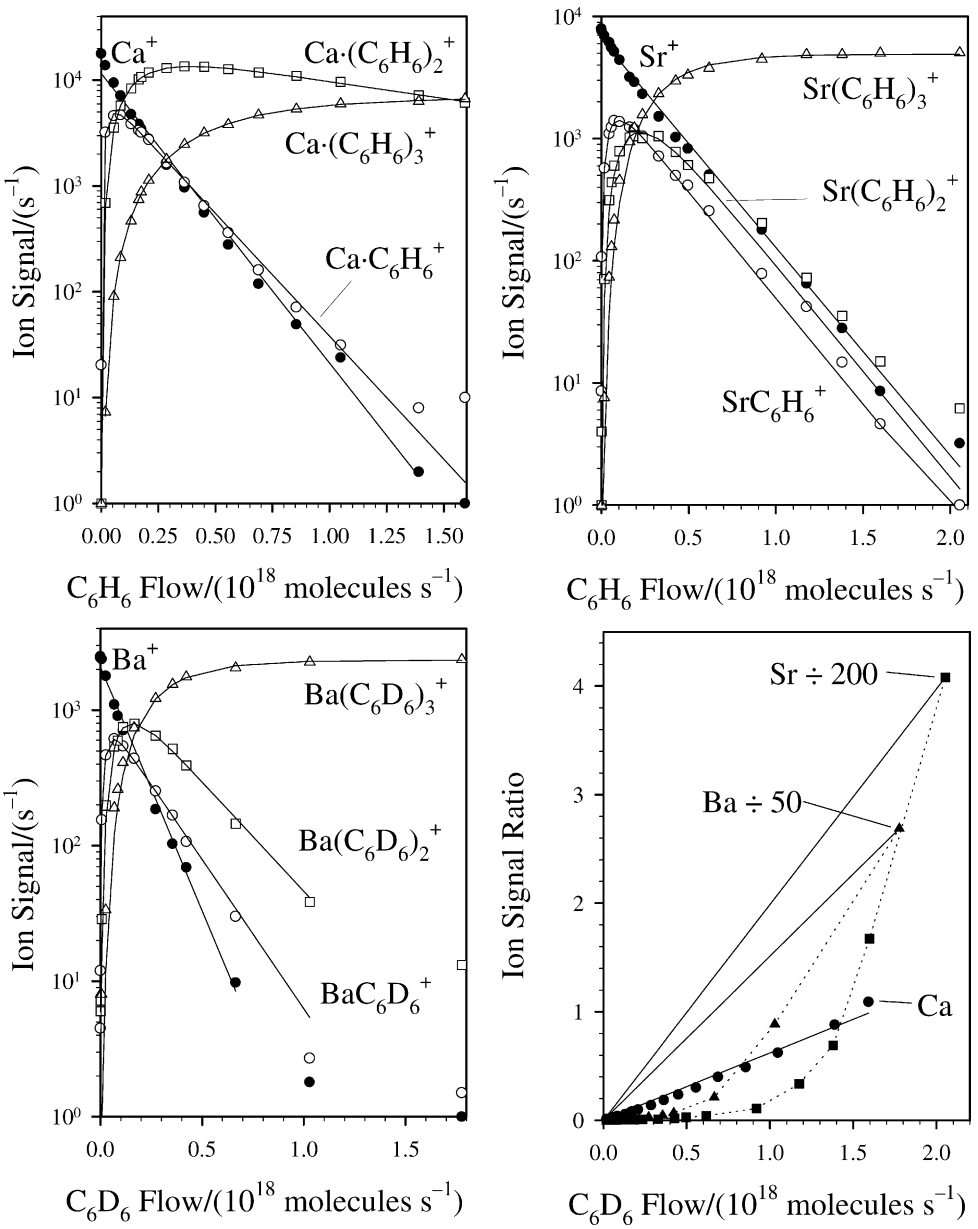

Fig. 2. Reaction profiles for the reactions of Ca^+, Sr^+, and Ba^+ with benzene to form $M(C_6H_6)_2^+$ clusters by sequential addition. Ions signal ratio-plots (lower right) show the variation in the ratio $M(C_6H_6)_3^+/M(C_6H_6)_2^+$ with the benzene flow. Only calcium exhibits equilibrium kinetics upon addition of a third benzene molecule to Ca^+.

10^{-10} cm^3 molecule^{-1} s^{-1} for Ca^+ (first two), 2.6, 6.1, and 6.0×10^{-10} cm^3 molecule^{-1} s^{-1} for Sr^+ and 6.2, 7.5, and 6.4×10^{-10} cm^3 molecule^{-1} s^{-1} for Ba^+. The higher number of added benzene molecules to these Group 2 ions can be attributed to their larger size.

2.2. Equilibrium kinetics and thermodynamics

The first addition of benzene was observed to achieve equilibrium for the Group 1 ions K^+, Rb^+ and Cs^+. A large number of the higher-order benzene addition reactions were also observed to approach and attain equilibrium under the SIFT conditions that were employed. The approach of equilibrium was monitored by tracking $I(M(C_6H_6)_2^+)/I(MC_6H_6^+)$ and $I(M(C_6H_6)_3^+)/I(M(C_6H_6)_2^+)$ with added benzene. The attainment of linear dependence is a signature of the attainment of equilibrium because $K_{eq} = [M(C_6H_6)_2^+)]/([MC_6H_6^+][C_6H_6])$ for reaction (2) and $K_{eq} = [M(C_6H_6)_3^+)]/([M(C_6H_6)_2^+] \times [C_6H_6])$ for reaction (3). At equilibrium $I(M(C_6H_6)_2^+)/I(MC_6H_6^+) = K_{eq}\,[C_6H_6]$ for reaction (2) and $I(M(C_6H_6)_3^+)/I(M(C_6H_6)_2^+) = K_{eq}\,[C_6H_6]$ for reaction (3). Fig. 1, for example, shows the attainment of equilibrium for the second addition of benzene in the reactions of the Group 14 ions Ge^+, Sn^+ and Pb^+. Fig. 2 shows the failure to achieve equilibrium, even for the addition of a third molecule of benzene, in the case of the reactions involving the Group 2 ions Sr^+ and Ba^+, while Ca^+ (a smaller ion) dose achieves equilibrium on the addition of the third benzene. Fig. 3 shows the attainment of equilibrium for each of the two benzene additions observed with In^+ together with a measurement of the multi-collision induced dissociation of $In(C_6H_6)_2^+$ and $InC_6H_6^+$. The relative binding energies are clearly apparent with the second benzene molecule being bound much less strongly than the first.

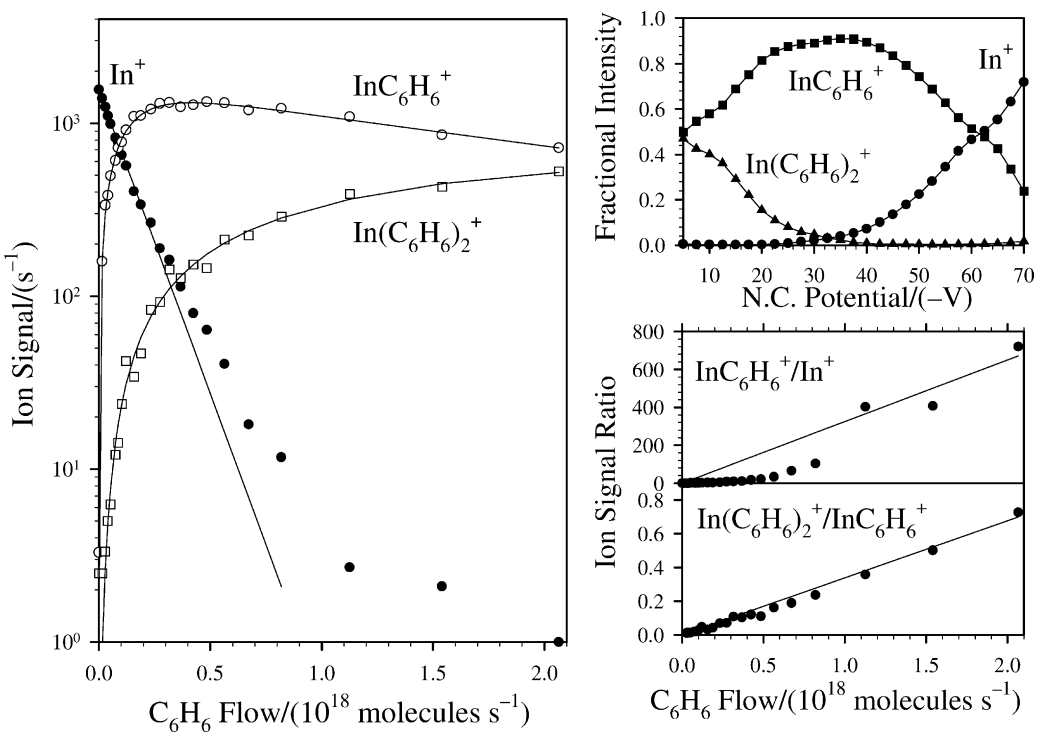

Fig. 3. Equilibrium kinetics (left) for the clustering of benzene onto In^+ showing the sequential formation of $In(C_6H_6)_2^+$. Ion signal ratio-plots (right, lower) for the determination of reaction equilibrium constants and multi-collision induced dissociation (right, upper) of $In(C_6H_6)_2^+$ and $InC_6H_6^+$ to form bare In^+.

Table 2
Comparison of experimental and computed reaction free energies changes (ΔG°_{298} in kcal mol^{-1}) for clustering reactions that exhibited equilibrium-like kinetics

Ion	ΔG° experimental[a]			ΔG° computed[b]	
	1st	2nd	3rd	1st	2nd
K^+	−9.5	−8.5		−8.3	−6.1
Rb^+	−8.6	−7.1		−6.2	−5.3
Cs^+	−8.6	–			
Ca^+	≤−15	−12.8	−9.2	−18.7	−9.1
Sr^+	≤−15	≤−15	≤−15	−14.3	−9.5
Ba^+	≤−15	≤−15	≤−12		
Zn^+	≤−15	−11.1		−36.0	−11.2
Cd^+	≤−15	−10.0		−24.1	−7.5
Hg^+	e^- trans				
Ga^+	≤−15	−9.1		−23.4	−6.3
In^+	≤−15	−9.2		−16.8	−5.5
Tl^+	≤−12	−9.3			
Ge^+	≤−15	−9.4		−41.1	−6.7
Sn^+	≤−15	−10.4		−29.3	−6.8
Pb^+	≤−13	−9.7			
As^+[c]	≤−15			−59.1	−6.1
Sb^+	≤−15	−9.7		−42.4	−7.1
Bi^+	≤−13	−10.1			
Te^+	≤−15	−9.2		−23.1	−5.4

[a] Accuracy estimated to be better than 0.2 kcal mol^{-1}.
[b] See Tables 3 and 4.
[c] Weak signal observed for $As(C_6H_6)_2^+$.

The measured equilibrium constants provide values for the standard free energy change, ΔG°, for the benzene additions since $\Delta G^\circ = -RT\ln(K_{eq})$. The values of ΔG° determined in this study at 296 K are summarized in Table 2. The dynamic range of the instrument prevents the measurement of reaction standard free energy changes more negative than −15 kcal mol^{-1}.

For the first addition of benzene, reaction (1), values of ΔG° were obtained only for the Group 1 ions K^+, Rb^+ and Cs^+ and were in the range −8.6 to −9.5 kcal mol^{-1}. Equilibrium was not achieved for the addition of benzene to the remaining main-group ions, $\Delta G^\circ = -12$ kcal mol^{-1}. For the two additions of benzene to K^+ comparisons can be made with high-pressure ion source mass spectrometry measurements previously reported by Sunner et al. [5]. Using their experimentally determined values of −22.4 and −25.1 cal K^{-1} mol^{-1} for ΔS°, we obtain values of −16.1 and −15.9 kcal mol^{-1} for ΔH° from our values of ΔG° for the addition of the first and the second molecule of benzene, respectively. Our absolute values for ΔH° are about 10% lower than the corrected values of −18.3 and −17.0 kcal mol^{-1} obtained from van't Hoff plots by Sunner et al [5]. For the first addition of benzene slightly better agreement is found with the collision-induced dissociation experiments of Amicangelo and Armentrout [7], who have reported a value of −17.7±1.0 kcal mol^{-1} for ΔH°_{298} derived from a measurement of D_0 and a computed thermal correction. For the addition of one benzene molecule to Rb^+, Amicangelo and Armentrout [7] reported a value for ΔG°_{298} of −10.1 kcal mol^{-1} that is 17% more negative than our value. It should also be noted that best high level theoretical values for the binding enthalpies at 298 for K^+(benzene) = −20.1±0.4 kcal mol^{-1} and Rb^+(benzene) = −16.4± 0.2 kcal mol^{-1} reported by Feller et al. [10] are systematically higher in absolute value than the values of −14.6 and −12.5 kcal mol^{-1}, respectively, obtained here using B3LYP density-functional theory.

For the second addition of benzene, reaction (2), values of ΔG° were obtained for Groups 1, 12, 13, 14, 15 and 16 ions and were in the range from −7.1 to −11.2 kcal mol^{-1} (see Table 2). A value of $\Delta G^\circ = -9.2$ kcal mol^{-1} was obtained for Ca^+ for the third addition of benzene, reaction (3). However, equilibria were not observed with the Group 2 ions Sr^+ and Ba^+, presumably because $\Delta G^\circ \leq -15$ kcal mol^{-1}. In the case of K^+ and Rb^+, good agreement is found for the second benzene addition with the collision-induced dissociation experiments of Amicangelo and Armentrout [7] who have reported values of −6.0 and −4.7 kcal mol^{-1}, respectively for ΔG°_{298}. These values are within 2 and 11% of our values of −6.1 and −5.3 kcal mol^{-1}, respectively.

2.3. Computed energies and structures

Ion structures, reaction enthalpies, and reaction free energies were computed for K^+, Ca^+, Zn^+ through Se^+, Rb^+, Sr^+ and Cd^+ through Te^+ binding with

Table 3
Computed structures for $MC_6H_6^+$ and enthalpies, entropies and free energies for reactions of the type $M^+ + C_6H_6 \rightarrow MC_6H_6^+$ at the B3LYP/DZVP level of theory

Metal ion	Coordination	C–C[a]	M^+–C[b]	$q(M^+)$[c]	ΔH°_{298} (kcal mol^{-1})	ΔG°_{298} (kcal mol^{-1})	ΔS°_{298} (cal K^{-1} mol^{-1})
K^+	η_6	1.404	3.310	0.89	−14.6	−8.3	−21.1
Rb^+	η_6	1.403	3.508	0.91	−12.5	−6.2	−21.1
Ca^+	η_6	1.406	2.976	0.74	−25.3	−18.7	−22.1
Sr^+	η_6	1.405	2.852	0.78	−21.1	−14.3	−22.8
Zn^+	η_6	1.410	2.631	0.48	−41.9	−36.0	−19.8
Cd^+	η_6[d]	1.408	2.699, 3.413	0.64	−28.0	−24.1	−13.1
Ga^+	η_6	1.407	2.839	0.55	−30.6	−23.4	−24.1
In^+	η_6	1.406	3.079	0.66	−23.7	−16.8	−23.0
Ge^+	η_3	1.411	2.348, 3.383	0.44	−47.2	−41.1	−20.5
Sn^+	η_3	1.409	2.626, 3.628	0.55	−35.0	−29.3	−19.1
As^+	η_2	1.415	2.291, 3.606	0.39	−65.3	−59.1	−20.8
Sb^+	η_2	1.411	2.580, 3.850	0.49	−48.0	−42.4	−18.8
Se^+	η_6	1.410	3.022	0.45	−43.0	−36.6	−21.5
Te^+	η_6	1.408	3.274	0.58	−29.3	−23.1	−20.8

[a] C–C bond distance in Å. When coordination is η_2 or η_3, this is the average C–C bond distance.
[b] M^+–C bond distance in Å. When two numbers are listed, they correspond to the shortest and longest M^+–C separation in an η_2 or η_3 cluster.
[c] Mulliken population analysis, charge q in esu.
[d] Slightly offset from center.

one and two benzene molecules. The heavier elements were not computed because of basis-set limitations and the need for relativistic corrections. Selected structural parameters for the half- and full- sandwich along with reaction enthalpies, entropies, and free energies for the clustering reaction to produce these species are reported in Tables 3 and 4, respectively. Also given are the separations between M^+ and a C atom on benzene. We note here that the high level theories applied by Feller et al. [10] that predicts stronger bonding in K^+(benzene) and Rb^+(benzene) also predicts shorter M^+–C distances (shorter by ca. 0.2 and 0.1 Å for K^+(benzene) and Rb^+(benzene), respectively).

Table 2 shows that the computed reaction free energies are systematically more positive than those obtained experimentally, the mean and standard deviation of the difference being 2.5 and 1.1 kcal mol^{-1}, respectively. Notably the computed free energy change for production of $Zn(C_6H_6)_2^+$ lies outside 1σ for this systematic trend at 2.4σ. This discrepancy for Zn arises from a notable increase in computed reaction enthalpy for the full-sandwich of Zn^+. Possible explanations for this could include benzene–benzene interaction in the tilted sandwich structure and substantial electron transfer from the benzene rings to the zinc center, remembering that the ionization energy of Zn is larger than that of benzene.

The relative magnitudes of the first and second ligation free energies measured for K^+ and Rb^+ are reproduced by theory. The computed free energies for the first addition of benzene for all but the Group 1 ions are very negative, in the range of −14.3 to −59.1 kcal mol^{-1}, and so account for our failure to observe equilibrium experimentally for this ligation step. Both our experiments and theory show a large decrease in the absolute free energy change for the addition of the second molecule of benzene, again except for the Group 1 cations which have a rare-gas electronic configuration and so are expected to interact with benzene in a completely electrostatic fashion.

Table 4
Computed structures for $M(C_6H_6)_2^+$ and enthalpies, entropies and free energies for reactions of the type $MC_6H_6^+ + C_6H_6 \rightarrow M(C_6H_6)_2^+$ at the B3LYP/DZVP level of theory

Metal ion	Coordination	C–C[a]	M^+–C[b]	$q(M^+)$[c]	ΔH°_{298} (kcal mol^{-1})	ΔG°_{298} (kcal mol^{-1})	ΔS°_{298} (cal K^{-1} mol^{-1})
K^+	η_6 eclipsed	1.403	3.334	0.78	−12.4	−6.1	−21.1
Rb^+	η_6 eclipsed	1.403	3.5308	0.82	−10.2	−5.3	−16.4
Ca^+	η_6 eclipsed	1.404	3.061	0.61	−15.7	−9.1	−22.1
Sr^+	η_6 eclipsed	1.404	3.218	0.64	−14.7	−9.5	−17.4
Zn^+	η_6 tilted[d]	1.405	2.63, 3.24	0.37	−17.9	−11.2	−22.5
Cd^+	η_6 staggered[e]	1.405	3.02, 3.30	0.55	−13.3	−7.5	−19.5
Ga^+	η_6 eclipsed	1.404	3.067	0.53	−12.5	−6.3	−20.8
In^+	η_6 eclipsed	1.404	3.283	0.60	−10.8	−5.5	−17.8
Ge^+	η_3 eclipsed	1.405	2.704, 3.500	0.45	−12.2	−6.7	−18.4
Sn^+	η_3 staggered[f]	1.404	2.91, 3.73	0.51	−12.6	−6.8	−19.5
As^+	η_2 eclipsed	1.406	2.659, 3.720	0.41	−11.3	−6.1	−17.4
Sb^+	η_2 eclipsed	1.406	2.879, 3.879	0.47	−12.5	−7.1	−18.1
Se^+	η_6 eclipsed	1.406	3.1409	0.38	−14.7	−9.7	−16.8
Te^+	η_6 eclipsed	1.405	3.437	0.49	−13.6	−7.4	−20.8

[a] C–C bond distance in Å. When coordination is η_2 or η_3, this is the average C–C bond distance.
[b] M^+–C bond distance in Å. When two numbers are listed, they correspond to the shortest and longest M^+–C separation in an η_2 or η_3 cluster.
[c] Mulliken population analysis, charge q in esu.
[d] Each benzene ring is tilted 16° from a parallel geometry and staggered 10°.
[e] Staggered 12°.
[f] Staggered 30°.

Our results obtained with multi-collision induced dissociation (MCID) experiments are in general agreement with computations but cannot provide accurate thermochemical information from the measured thresholds. The observed sequences of dissociation are consistent with theory as are their differences in the onset voltage. For example, as shown in Fig. 1, the $In(C_6H_6)_2^+$ cluster is collisionally dissociated in a sequential manner at −16 and −58 V respectively, to ultimately produce bare In^+. Computations predict the respective sequential dissociation enthalpies to be 10.8 and 23.7 kcal mol^{-1}. A larger difference in sequential dissociation enthalpy is computed for $Ge(C_6H_6)_2^+$, 12.2 and 47.2 kcal mol^{-1}, respectively, and only the first dissociation is observed experimentally at −16 V. The $GeC_6H_6^+$ ion could not be dissociated at the highest available nose-cone voltage, −70 V.

Structures for half- and full-sandwich clusters of Rb^+, Ge^+, and As^+ are shown in Fig. 4. The peri-

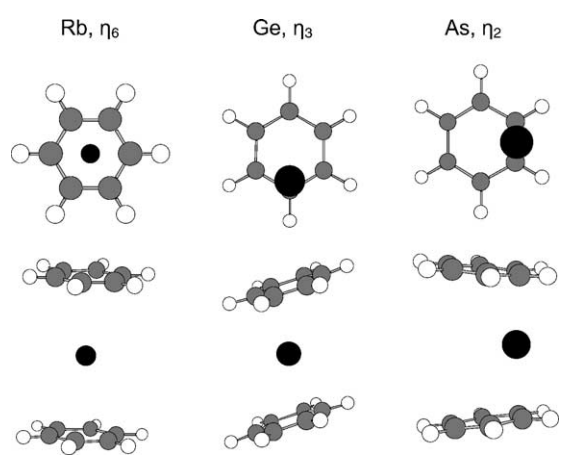

Fig. 4. Structures for one and two benzene molecules bonded to $Rb^+(\eta_6)$, $Ge^+(\eta_3)$ and $As^+(\eta_2)$. Bond distances are reported in Tables 3 and 4.

odic trend in the full- and half-sandwich structures evident in Table 4 can be rationalized in terms of the valence shell electron configuration (VSEC) of the metal cation. Examining the third row elements, we see that K^+ and Ga^+ have spherical VSECs: [Ar] and $4s^2$, respectively, and are both η_6 coordinated. Ca^+ and Zn^+ both have spherical $4s^1$ VSECs and are also η_6 coordinated. Interestingly, Ca^+ and Zn^+ are more strongly and closely bound to the benzene ligand than K^+ and Ga^+, respectively, suggesting that the unpaired 4s electron (in Ca^+ and Zn^+) is participating, to some degree, in a covalent bond with the benzene ligands. Ge^+ has an VSEC of $4p^1$ and is η_3 coordinated with the metal lying directly above a carbon atom in the half-sandwich complex. As^+ has a VESC of $4p^2$ and is η_2 coordinated. Of the third row elements studied computationally, the Arsenic half-sandwich has the most negative reaction enthalpy and the full-sandwich has the most negative sum of first and second clustering enthalpies. With the exception of Cd^+ (which possesses a broad minimum covering much of the π-cloud of the benzene ring) these trends are repeated in the clusters composed of fourth row metals. The energy difference between C_{6v} $CdC_6H_6^+$ and that in which cadmium is bound almost vertically over a carbon is only 0.1 kcal mol^{-1}.

Computations generally revealed that η_6 sandwich clusters prefer an eclipsed conformation versus a staggered conformation. However, a study of the barrier height for internal rotation in the $Ga(C_6H_6)_2^+$ cluster revealed this quantity to be a scant 0.02 kcal mol^{-1}. Furthermore, for the $Zn(C_6H_6)_2^+$ cluster a canted or tilted η_4 structure was found to be the ground state structure. In this complex, each of the benzene rings is tilted 16° from parallel and staggered 10°. Compared to the eclipsed D_{6h} conformer, the tilted structure was 0.5 kcal mol^{-1} lower in energy.

The extent of electron transfer from the benzene ligands to the metal cation is explored empirically in Fig. 5 in two separate correlations. Fig. 5(a) shows the relationship between the charge on the metal atom and the strength of the interaction of the metal ion with the first and second benzene additions. For the first addition of benzene, the charge on the metal decreases asymptotically to approximately 0.4 esu with increasing binding energy. The second addition introduces only a relatively minor perturbation. Fig. 5(b) displays the variation of the average C–C bond length in the benzene ligands as a function of the charge retained on the metal ion. The C–C bond length reflects the extent of electron transfer out of bonding orbitals and into antibonding orbitals on the benzene ligand. Again, the C–C bond length in the half-sandwich is strongly sensitive to the charge on the atomic ion.

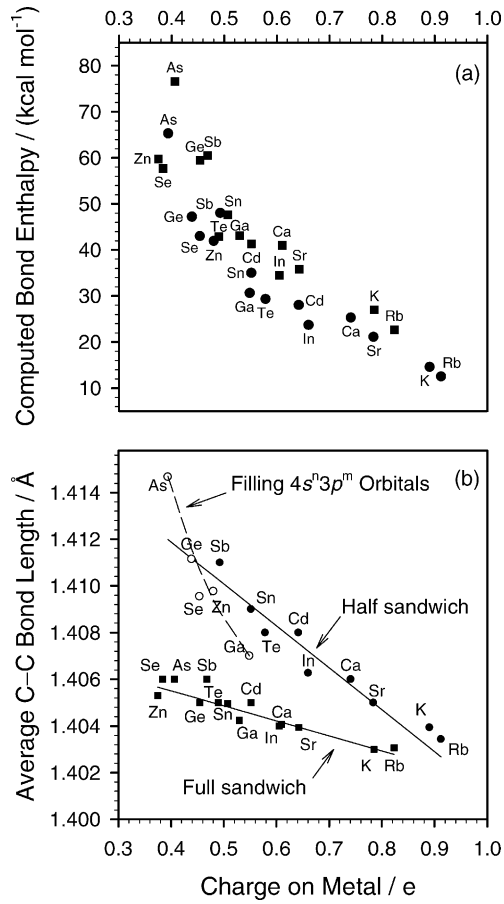

Fig. 5. Variations of computed total bond enthalpies (a) and average C–C bond length (b) with the total atomic charge on the metal (Mullikan population analysis). The solid circles and squares correspond to half-sandwich and full-sandwich structures, respectively. The open circles in (b) highlight the continuous fourth-period sequence for the half-sandwiches of Zn through Se which possibly exhibits a steeper correlation.

Addition of the second benzene leads to a decrease in the average C–C bond length, presumably because of the resulting competition for the atomic charge.

Of special note is the behaviour observed with As^+ and Ge^+. For these two ions, computations predict that the metal becomes more positive with the addition of the second benzene ligand whereas in all other cases the metal becomes less positive. In transiting from bare to half- to full-sandwich clusters, K^+ and Rb^+ lose positive charge in two equal steps of about 0.1 esu, suggesting a fully electrostatic interaction.

3. Conclusions

Both kinetic and equilibrium measurements have been performed for the sequential clustering of benzene to 20 main-group atomic cations. Under the SIFT operating conditions, benzene clusters to 18 of the 20 atomic ions investigated with only two, Hg^+ and I^+, reacting exclusively by electron transfer. Only the reaction with Zn^+ exhibits both electron transfer and clustering. With the exception of Hg^+ and I^+, all of the main-group atomic ions investigated were observed to add two benzene molecules at room temperature in helium buffer at 0.35 Torr, but the larger Group 2 (s^1) ions Ca^+, Sr^+ and Ba^+ added three benzene molecules in rapid succession.

Both the experiments and theory show a large change in free energy for the first ligation with benzene, except for the Group 1 cations that have a rare-gas electronic configuration. Values for the free energies of ligation determined experimentally are ca. $-9\,\mathrm{kcal\,mol^{-1}}$ for the Group 1 cations and $<-12\,\mathrm{kcal\,mol^{-1}}$ for all other cations. For the ligation of the latter cations B3LYP level of theory predicts changes in free energy from -14.3 (for Sr^+(benzene) formation) to $-59.1\,\mathrm{kcal\,mol^{-1}}$ (for As^+(benzene) formation). Comparisons with higher-level theory results for K^+(benzene) and Rb^+(benzene) suggest that the B3LYP results slightly underestimate enthalpies of benzene ligation for these two adduct ions.

Both our experiments and theory also show a large decrease in the absolute free energy change for the addition of the second molecule of benzene; the latter lie in the range from -5 to $-11\,\mathrm{kcal\,mol^{-1}}$. Experimentally, the Group 2 cations Cr^+, Sr^+ and Ba^+ exhibited the largest absolute free energies of ligation for the second addition of benzene with values of -12.8, ≤ -15 and $\leq -15\,\mathrm{kcal\,mol^{-1}}$, respectively.

The B3LYP level of theory also can provide insight into the structures of the half- and full-sandwich benzene clusters. η_6, η_3 and η_2 structures are identified for the full-sandwich. Periodic trends in these structures are rationalized in terms of the valence shell electron configuration (VSEC) of the metal cation.

Acknowledgements

Continued financial support from the Natural Sciences and Engineering Research Council of Canada is greatly appreciated. Also, we acknowledge support from the National Research Council, the Natural Science and Engineering Research Council and MDS SCIEX in the form of a Research Partnership grant. As holder of a Canada Research Chair in Physical Chemistry, Diethard K. Bohme thanks the contributions of the Canada Research Chair Program to this research.

References

[1] D.A. Dougherty, Science 271 (1996) 163.
[2] J. Cernicharo, A.M. Heras, A.G.G.M. Tielens, J.R. Pardo, F. Herpin, M. Gulin, L.B.F.M. Waters, Astrophys. J. 346 (2001) L123.
[3] D.K. Bohme, Chem. Rev. 92 (1992) 1487.
[4] R.L. Wooden, J.L. Beauchamp, J. Am. Chem. Soc. 100 (1978) 501.
[5] J. Sunner, K. Nishizawa, P. Kebarle, J. Phys. Chem. 85 (1981) 1814.
[6] B.C. Guo, J.W. Purnell, A.W. Castleman Jr., Chem. Phys. Lett. 168 (1990) 155.
[7] J.C. Amicangelo, P.B. Armentrout, J. Phys. Chem. A 104 (2000) 11420.
[8] J.H. El-Nakat, I.G. Dance, K.J. Fisher, G.D. Willett, Polyhedron 13 (1994) 409.
[9] J.B. Nicholas, B.P. Hay, D.A. Dixon, J. Phys. Chem. A 103 (1999) 1394.
[10] D. Feller, D.A. Dixon, J.B. Nicholas, J. Phys. Chem. A 104 (2000) 11414.
[11] S. Arulmozhitaja, T. Fujii, H. Tokiwa, Int. J. Mass Spectrom. 250 (1999) 237.

[12] T. Fujii, S. Arulmozhitaja, Int. J. Mass Spectrom. 198 (2000) 15.
[13] G.I. Mackay, G.D. Vlachos, D.K. Bohme, H.I. Schiff, Int. J. Mass Spectrom. Ion Phys. 36 (1980) 259.
[14] A.B. Raksit, D.K. Bohme, Int. J. Mass Spectrom. Ion Processes 55 (1983/84) 69.
[15] G.K. Koyanagi, V.V. Lavrov, V.I. Baranov, D. Bandura, S.D. Tanner, J.W. McLaren, D.K. Bohme, Int. J. Mass Spectrom. 194 (2000) L1.
[16] G.K. Koyanagi, V.I. Baranov, S.D. Tanner, D.K. Bohme, J. Anal. At. Spectrom. 15 (2000) 1207.
[17] V. Baranov, D.K. Bohme, Int. J. Mass Spectrom. Ion Processes 154 (1996) 71.
[18] M.J. Frisch, G.W. Trucks, H.B. Schlegel, G.E. Scuseria, M.A. Robb, J.R. Cheeseman, V.G. Zakrzewski, J.A. Montgomery, Jr., R.E. Stratmann, J.C. Burant, S. Dapprich, J.M. Millam, A.D. Daniels, K.N. Kudin, M.C. Strain, O. Farkas, J. Tomasi, V. Barone, M. Cossi, R. Cammi, B. Mennucci, C. Pomelli, C. Adamo, S. Clifford, J. Ochterski, G.A. Petersson, P.Y. Ayala, Q. Cui, K. Morokuma, D.K. Malick, A.D. Rabuck, K. Raghavachari, J.B. Foresman, J. Cioslowski, J.V. Ortiz, A.G. Baboul, B.B. Stefanov, G. Liu, A. Liashenko, P. Piskorz, I. Komaromi, R. Gomperts, R.L. Martin, D.J. Fox, T. Keith, M.A. Al-Laham, C.Y. Peng, A. Nanayakkara, C. Gonzalez, M. Challacombe, P.M.W. Gill, B. Johnson, W. Chen, M.W. Wong, J.L. Andres, C. Gonzalez, M. Head-Gordon, E.S. Replogle, J.A. Pople, Gaussian 98, Revision A.7, Gaussian, Inc., Pittsburgh PA, 1998.
[19] A.D. Becke, J. Chem. Phys. 98 (1993) 5648.
[20] C. Lee, W. Yang, R.G. Parr, Phys. Rev. B 37 (1988) 785.
[21] B. Miehlich, A. Savin, H. Stoll, H. Preuss, Chem. Phys. Lett. 157 (1989) 200.
[22] N. Godbout, D.R. Salahub, J. Andzelm, E. Wimmer, Can. J. Chem. 70 (1992) 560.
[23] S.G. Lias, in: P.J. Linstrom, W.G. Mallard (Eds.), NIST Chemistry WebBook, NIST Standard Reference Database Number 69, July 2001, National Institute of Standards and Technology, Gaithersburg MD, 20899 (http://webbook.nist.gov).
[24] M.A. Baig, J. Phys. B 16 (1983) 1511.
[25] L. Minnhagen, Ark. Phys. (Stockholm) 21 (1962) 415.
[26] C.M. Brown, S.G. Tilford, M.L. Ginter, J. Opt. Soc. Am. 65 (1975) 1404.
[27] T. Su, W.J. Chesnavich, J. Chem. Phys. 76 (1982) 5183.